A Time-Domain Algorithm for the Analysis of Second-Harmonic Generation in Nonlinear Optical Structures

Mohammad A. Alsunaidi, Husain M. Masoudi, and John M. Arnold

***Abstract*—A time-domain simulator of integrated optical structures containing second-order nonlinearities is presented. The simulation algorithm is based on nonlinear wave equations representing the propagating fields and is solved using the finite-difference time-domain method. The simulation results for a continuous-wave operation are compared with beam propagation method simulations showing excellent agreement for the particular examples considered. Because the proposed algorithm does not suffer from the inaccuracies associated with the paraxial approximation, it should find application in a wide range of device structures and in the analysis of short-pulse propagation in second-order nonlinear devices.**

***Index Terms*—Finite-difference time-domain (FDTD) method, modeling, nonlinear wave propagation, second-harmonic generation.**

I. Introduction

With the advent of fast and powerful computers, detailed numerical simulation of accurate models representing the physical phenomena inside nonlinear optical devices has become efficient and reliable. For example, the beam propagation method (BPM) has been successfully used in the analysis of second-harmonic generation (SHG) in a number of nonlinear optical structures [1]. This method is relatively flexible and computationally efficient. However, the formulation of the fields provides only the steady-state behavior. It is also limited to modeling devices where the primary flow of energy is along a single principal direction. These facts severely limit the applicability of the method.

The finite-difference time-domain (FDTD) method has also been successfully applied in a variety of problems involving electromagnetic radiation and propagation in linear as well as nonlinear structures (for example [2]–[3]). This method provides comprehensive solutions of time-domain models without the simplifying assumptions that limit the application of the BPM. The main, and serious, drawback of the FDTD method, however, is the intense consumption of computational power for typical time-domain simulations. A compromise between the amount of data needed for analysis and the available computer resources has to be established.

Manuscript received September 9, 1999; revised November 30, 1999. This work was supported by the British Council.

M. A. Alsunaidi and H. M. Masoudi are with the Department of Electrical Engineering, King Fahd University of Petroleum and Minerals, Dhahran 31261 Saudi Arabia (e-mail: msunaidi@kfupm.edu.sa).

J. M. Arnold is with the Department of Electronics and Electrical Engineering, University of Glasgow, Glasgow, U.K.

Publisher Item Identifier S 1041-1135(00)02817-2.

In this letter, we present a new time-domain formulation of the SHG in nonlinear optical waveguides with a suitable FDTD solution. The equations representing the propagating fields are derived using a nonlinear wave equation such that the problem is reduced to an equivalent scalar problem. In planar waveguides, a TE-polarized fundamental mode can couple to a TM-polarized second-harmonic mode through an appropriate tensor coefficient of the nonlinear susceptibility. Although limited to such cases, this class of problems covers a significant number of practical applications such as GaAs-based planar waveguides. In this case, both fields can be represented by equivalent wave equations. This new formulation of the SHG problem offers great advantages over both the classical BPM technique and the vectorial FDTD method. While it completely accounts for the wave-medium interactions (e.g., nonlinear coupling, reflections, scattering, transients, etc.), it avoids the limitations associated with conventional asymptotic behavior and paraxial propagation. On the other hand, it provides an efficient method for the time-domain characterization of nonlinear optical structures by focusing on such quantities as beam intensity, nonlinear depletion and phase shift, characteristic lengths, etc., in which detailed analysis of the field components is not necessary. For a two-dimensional (2-D) SHG problem, for example, the proposed time-domain algorithm solves for only two fields; the fundamental field and the second-harmonic field. For the same problem, the conventional FDTD algorithm solves for three field components. In addition, it also intermediately evaluates the electric flux density components. The computational saving in this case is more than 50%. This fact makes the proposed formulation more attractive than the full-wave solution, especially when three-dimensional characterization of optical devices with typical dimensions is sought. In this way the proposed algorithm overcomes the limitations of computational intensity.

The new algorithm is capable of incorporating different techniques in the SHG process including quasi-phase matching (QPM), and it can simulate continuous-wave (CW) second-order nonlinear effects as well as operations with time-varying envelops. The amount of published work in this particular area is very limited, and to the best of our knowledge, no previous attempt for the analysis and validation of a FDTD-based solution was reported. For this reason, the simulation results of the new FDTD formulation will be compared with the CW BPM results for cases where the paraxial approximation is valid. Two examples involving second-harmonic generation in GaAs-based planar waveguides are presented in detail.

II. Formulations

The formulation of the fundamental and second-harmonic fields starts with the scalar wave equation []

$$\nabla^2 E = \mu_o \varepsilon_o n^2 \frac{\partial^2 E}{\partial t^2} + \mu_o \varepsilon_o \frac{\partial^2 P}{\partial t^2} \tag{1}$$

where E is the electric field intensity, P is the polarization given by $P_k = \chi^{(2)} E_i E_j$, n is the material refractive index, and $\chi^{(2)}$ is the dispersionless nonlinear susceptibility. Consider three different fields propagating at three different frequencies $E_1(\omega_1)$, $E_2(\omega_2)$, and $E_3(\omega_3)$ in a material exhibiting an instantaneous second-order nonlinearity

$$\nabla^2 E_1 = \mu_o \varepsilon_o n_1^2 \frac{\partial^2 E_1}{\partial t^2} + \mu_o \varepsilon_o \chi^{(2)}_{(\omega_1)} \frac{\partial^2 (E_2 E_3)}{\partial t^2} \tag{2}$$

$$\nabla^2 E_2 = \mu_o \varepsilon_o n_2^2 \frac{\partial^2 E_2}{\partial t^2} + \mu_o \varepsilon_o \chi^{(2)}_{(\omega 2)} \frac{\partial^2 (E_1 E_3)}{\partial t^2} \tag{3}$$

and

$$\nabla^2 E_3 = \mu_o \varepsilon_o n_3^2 \frac{\partial^2 E_3}{\partial t^2} + \mu_o \varepsilon_o \chi^{(2)}_{(\omega 3)} \frac{\partial^2 (E_1 E_2)}{\partial t^2}. \tag{4}$$

Equation (2) can be rewritten as

$$\nabla^2 E_1 = \mu_o \varepsilon_o n_1^2 \frac{\partial^2 E_1}{\partial t^2} + \mu_o \varepsilon_o \chi^{(2)}_{(\omega_1)} \cdot \left\langle E_2 \frac{\partial^2 E_3}{\partial t^2} + E_3 \frac{\partial^2 E_2}{\partial t^2} + 2 \frac{\partial E_2}{\partial t} \frac{\partial E_3}{\partial t} \right\rangle. \tag{5}$$

Similar manipulations can be done to (3) and (4). With $\omega_1 = \omega_2 = \omega$, $\omega_3 = \omega_1 + \omega_2 = 2\omega$, $\chi^{(2)} = \chi^{(2)}(\omega_1)/2 = \chi^{(2)}(\omega_3)$, and $E^f = E_1 = E_2$ and $E^s = E_3$, the following equations representing respectively the fundamental and the second-harmonic fields can be obtained:

$$\nabla^2 E^f = \mu_o \varepsilon_o n_f^2 \frac{\partial^2 E^f}{\partial t^2} + 2\mu_o \varepsilon_o \chi^{(2)} \cdot \left\langle E^f \frac{\partial^2 E^s}{\partial t^2} + E^s \frac{\partial^2 E^f}{\partial t^2} + 2 \frac{\partial E^f}{\partial t} \frac{\partial E^s}{\partial t} \right\rangle \tag{6}$$

and

$$\nabla^2 E^s = \mu_o \varepsilon_o n_s^2 \frac{\partial^2 E^s}{\partial t^2} + 2\mu_o \varepsilon_o \chi^{(2)} \cdot \left\langle E^f \frac{\partial^2 E^f}{\partial t^2} + \frac{\partial E^f}{\partial t} \frac{\partial E^f}{\partial t} \right\rangle. \tag{7}$$

III. FDTD Solutions and Numerical Results

The discritization schemes and the time-stepping algorithm for the two fields have to be arranged carefully. For this reason, the semi-implicit FD scheme [3] is used to improve the overall accuracy and stability of the solution. In fact, using this scheme, the stability condition of the linear wave equation solution can be used even with strong nonlinearity. However, due to the coupling terms in the fundamental and second-harmonic field equations, the evaluation of the two fields at the same time step is not possible because knowledge of the updated value of E^s is required. To solve this problem, one can introduce a few iterations at each time step to find convergent values of the two fields. This approach, however, will increase the computational intensity of the algorithm. Alternatively, the two fields can be staggered in time such that the fundamental field leads the second harmonic by one time step and effectively decoupling the two fields in time. The value $E^{f(n+1)}$ is, thus, computed using the values of E^s at time instances n, $n-1$, and $n-2$. This technique is found to be more efficient, and the accuracy of the solution is enhanced if the time-step size is kept small. It should be pointed out, however, that when the algorithm is used to evaluate field envelops in CW simulations, the terms involving time derivatives of E^s in (6) can be neglected because they eventually equal to zero at steady state.

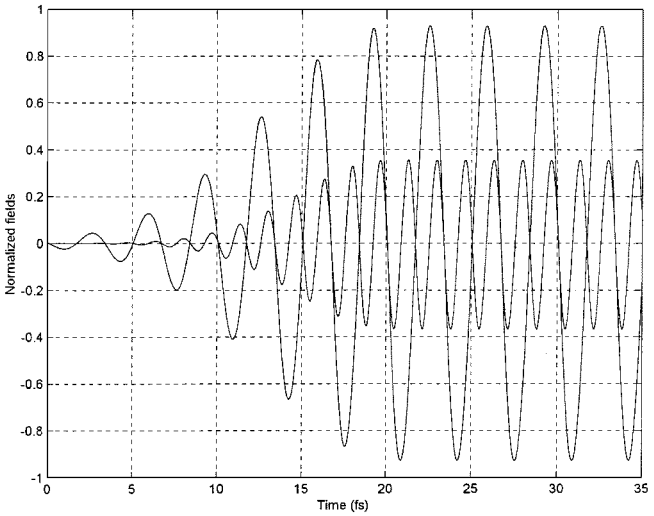

Fig. 1. Time-domain evolution of the fundamental and second-harmonic fields at an arbitrary point within the guiding layer of the asymmetric waveguide. The waveguide consists of a 2-μm-thick substrate ($n = 3.1$) and cladding ($n = 1.0$) layers and a 0.44-μm-thick guiding layer ($n_f = 3.605\,55$).

As a first example for the validation of the FDTD algorithm, a phase-matched case is considered. The structure used for the FDTD simulation is an asymmetric GaAs-based slab dielectric waveguide. The excitation field is a CW signal at a fundamental wavelength of $\lambda_f = 1.55$ μm and an amplitude of 1.0×10^9 V/m. The transverse profile of the excitation corresponds to the first guided mode at the given operating frequency with effective index $n_{\text{eff}} = 3.4078$. To facilitate the propagation of the first guided mode of the second-harmonic field at the same effective refractive index with $\lambda_s = 0.775$ μm (phase-matched condition), the value $n_s = 3.4778$ is chosen inside the guiding layer. The nonvanishing element of the nonlinear susceptibility tensor of the bulk GaAs is taken as $\chi^{(2)}_{\text{xyz}} = 200$ pm/V. This value is off the second-harmonic resonance with the band edge where absorption of the second-harmonic energy is negligible. The excitation signal is smoothly entered in the computation domain to avoid numerical reflections. A long simulation time corresponding to tens of cycles was allowed to ensure steady-state results. The mesh parameters were carefully chosen to effectively reduce numerical dispersion especially in the propagation direction (z axis). Several experiments showed that a resolution of $\Delta z = \lambda_s/100$ ensured convergence. The computation domain is terminated by second-order absorbing boundaries to enhance the accuracy of the solution and to allow for long simulation times.

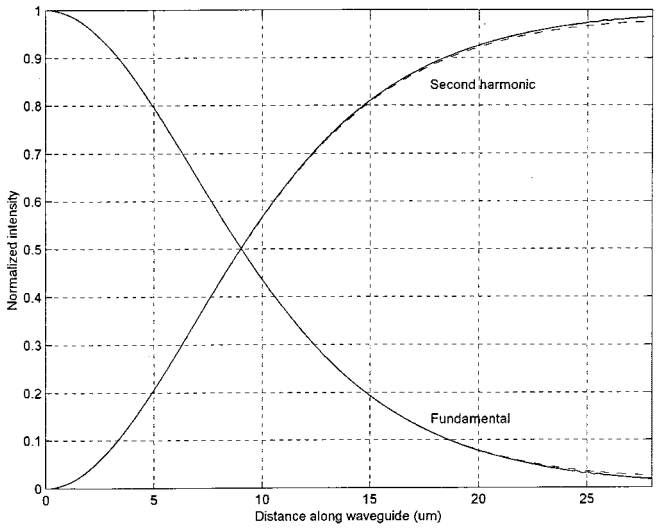

Fig. 2. Normalized intensities for the fundamental and second-harmonic fields along the waveguide. The FDTD results (solid) are compared with the BPM results (dashed).

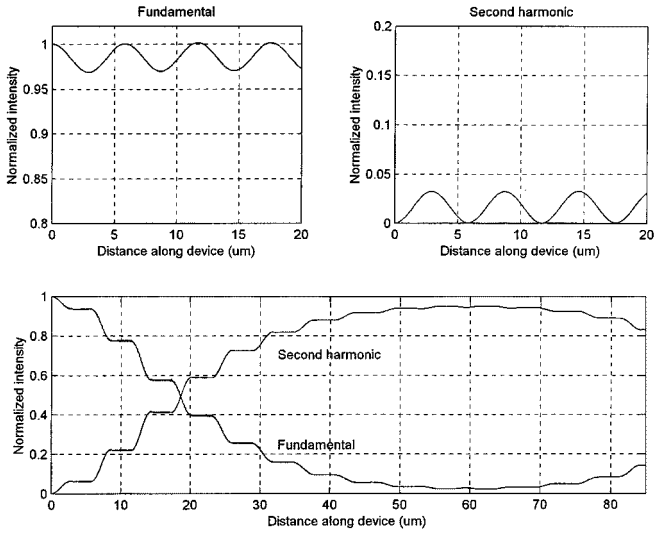

Fig. 3. Normalized intensities for the fundamental and second-harmonic fields along the waveguide for both: (top) non-QPM case and (bottom) QPM case.

The time-domain evolution of the fundamental and second-harmonic signals at an arbitrary point inside the guiding layer is shown in Fig. 1. It can be seen that the second-harmonic signal develops a frequency that is double the input frequency of the fundamental signal. It should be mentioned here that the transients that appear in the waveforms correspond to the smooth portion of the input signal used to feed the excitation into the computation window. The signals reach steady state after a number of cycles. The energy from the incident beam (fundamental) couples to the second harmonic on the first guided mode. Fig. 2 shows the FDTD steady-state normalized intensities corresponding to the fundamental and the second-harmonic signals (solid lines) along the waveguide. For comparison, 2-D BPM results (dashed lines) were also generated. The agreement between the two curves is excellent. It has to be noted that for this particular device structure, the effects of paraxial approximation and internal reflections are insignificant and hence the accuracy of the two methods is matching.

Further validation of the nonlinear FDTD algorithm involves the quasi-phase-matched (QPM) case. The QPM technique [] is a practical method of substantially increasing the second-harmonic power by effectively reducing the phase mismatch between the fundamental and the second-harmonic fields. This is achieved by modulating the nonlinear term in alternate half-periods in a corrugated structure. The amount of phase mismatch between the two fields is given by $\Delta k = 2k_o(n^s_{\text{eff}} - n^f_{\text{eff}})$. The amount of coupling between the fields can be controlled by adjusting the grating period and hence the amount of phase mismatch. Also, the grating period can be carefully chosen to ensure energy coupling to the first guided mode. Maximum power exchange is achieved by setting the corrugation period to be equal to the coherence length, which is defined as $L_C = 2\pi/\Delta k$. In this example, the same waveguide structure is used where the effective indexes corresponding to the first guided mode for both the fundamental and the second-harmonic fields are 3.4078 and 3.5347, respectively. A corrugated structure of period 5.85 μm, which is close to the coherence length, is used where the nonlinear susceptibility is periodically turned on for half a period and then off to $\chi^{(2)} = 0$ for the other half of the period. The fundamental and second-harmonic intensities are calculated as shown in Fig. 3. In this figure, the results for a non-QPM (no corrugations) case are also shown [Fig. 3(a)]. The oscillating curves demonstrate the case when $\Delta k \neq 0$. The intensity of the second harmonic increases over the first half-period and then decreases to zero over the rest of the period while the intensity is transferred back to the fundamental signal. The period of oscillation in the figure compares very well with the analytical value of L_C. The QPM simulation [Fig. 3(b)] clearly shows the improvement in the energy exchange between the two fields along the device compared to the non-QPM case.

IV. Conclusion

The application of the FDTD algorithm for modeling SHG in nonlinear optical devices has been demonstrated. Compared to the BPM, the result of the CW operation using the proposed FDTD algorithm is in close agreement. It does not, however, suffer from the inaccuracies associated with the paraxial approximation. As a consequence, the proposed algorithm finds application in a wider range of device geometries and structures. Also, being a time-domain technique, the presented algorithm has a great potential in the analysis of ultra-short-pulse propagation in nonlinear devices, which is the subject of current investigations.

Acknowledgment

The authors would like to acknowledge the support provided by King Fahd University of Petroleum and Minerals and the University of Glasgow.

References

[1] H. Masoudi and J. Arnold, "Modeling second order nonlinear effects in optical waveguides using a parallel-processing beam propagation method," *IEEE J. Quantum Electron.*, vol. 31, pp. 2107–2113, 1995.

[2] W. Huang, S. Chu, A. Goss, and S. Chaudhuri, "A scalar finite-difference time-domain approach to guided-wave optics," *IEEE Photon. Technol. Lett.*, vol. 3, pp. 524–526, 1991.

[3] A. Taflove, *Computational Electrodynamics: The Finite-Difference Time-Domain Method*. Norwood, MA: Artech House, 1995.

[4] M. M. Fejer, G. A. Magel, D. H. Jundt, and R. L. Byer, "Quasiphase-matched second-harmonic generation: Tuning and tolerances," *IEEE J. Quantum Electron.*, vol. 28, pp. 2631–2654, Nov. 1992.